Chapter 3
GALANT Antenna Design

In this chapter the design, simulation, construction and measurement of the new GALANT antenna are described in detail.

After the research carried out in the Chapter 2, a new geometry has been developed and adjusted in order to fulfil our objectives. This new antenna mixes almost all the features of the previous described antennas in order to optimize the results.

3.1. Introduction

The design of this new antenna tries to solve all the proposed objectives in one single structure. All the objectives are fulfilled with this new antenna structure, even the isolated feeding. The antenna geometry is composed of two stacked patches which radiate at both bands of interest. The RHCP is achieved using two ports for each patch. The two ports feeding a patch have a phase difference of 90° obtained just from one 90°-hybrid for each pair of ports.

Two types of feeding have been used: aperture coupled feeding for the low band and probe coupling for the high band. Moreover the dielectric permittivity has been chosen such that the radiation pattern fulfils our requirements.

At the beginning of the design process, the antenna is simulated in Ansoft Designer 4.0 in order to have an overview of the response of the antenna. Afterwards, all the design will be carried out in Ansoft HFSS 11 in order to have a precise simulation of the radiated fields.

3.2. Preliminary design

The preliminary design is carried out in Ansoft Designer 4.0. With this simulation application, the planar structures can be simulated relatively fast with an accurate results in input impedance and scattering parameters. Therefore is recommended to simulate the antenna first in Designer and afterwards in HFSS, since HFSS simulations are very time consuming.

3.2.1. Antenna geometry

The Figure 3.1 (a) presents the antenna geometry without the 90°-hybrids. At the beginning of the design, the antenna is simulated without the hybrids. The LF-Port and HF-Port are both composed of two feeding microstrip lines. These lines are fed with the same amplitude but with a 90° phase shift in order to achieve RHCP. It has to be pointed out the bigger patch is at the bottom; otherwise the big patch (low frequency band patch) could deform the radiation pattern of the small patch (high frequency band patch).

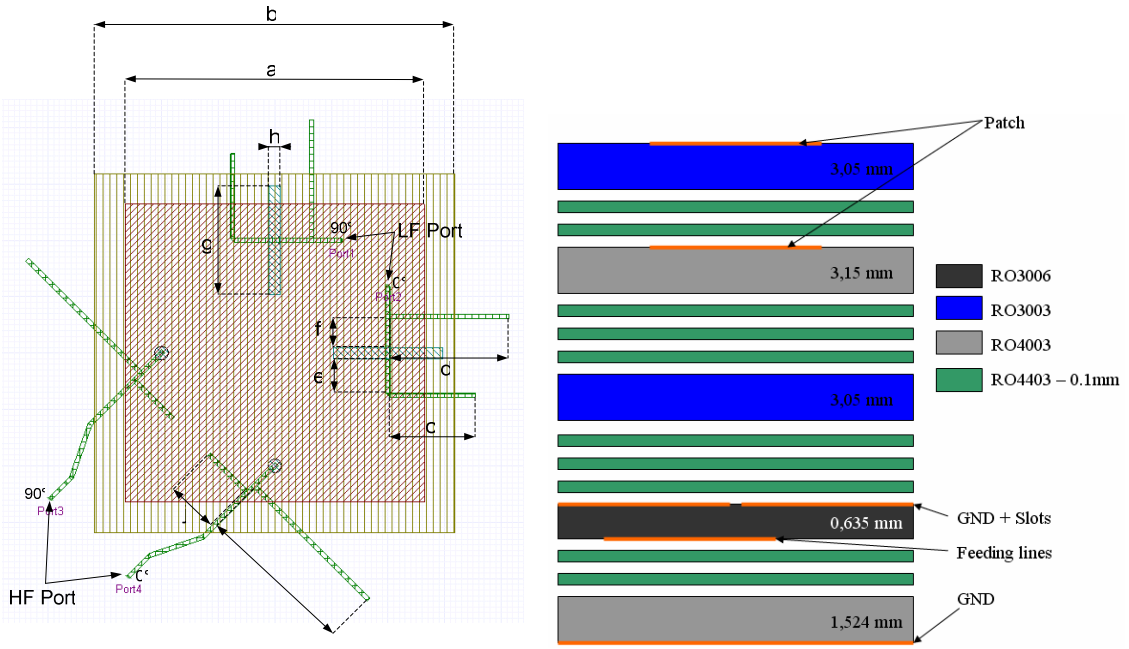

(a) (b)

Figure 3.1. (a) Top view and (b) side description of the antenna geometry

In the upper right part of the Figure 3.1 (a) presented above we can see the LF-Port feeding slots with the impedance matching stubs. Those stub lengths together with the slot length and position creates an impedance matching at 1.189 GHz for each feeding line.

The HF-Port is placed at the lower left part of the Figure 3.1 (a). This port is composed by the decoupling stubs, the impedance matching stubs and the probes that couple the energy to the upper patch. The decoupling stubs are those described with the dimension "i", and they are a $\lambda/4$ stubs with λ at 1.185 GHz. These stubs create a shortcircuit at 1.185GHz in the LF-Port feeding line in order to decouple this frequency and therefore isolate both LF and HF ports. The impedance matching stubs are those described with the dimension "j", matching the impedance of the feeding lines at 1.575 GHz. The probe via has a diameter of 0.8 mm and goes from the microstrip layer to the upper patch. The dimensions of the antenna are described in Table 3.1.

The Figure 3.1 (b) shows the layer description of the antenna. A total number of 3 different dielectric materials plus one glue material are used in this antenna. The dielectric Rogers RO3006 ($\varepsilon_r = 6.15$) is used in the microstrip feeding part in order to have a high

effective dielectric permittivity. Therefore the wavelength in the microstrip feeding is small with the intention of having a compact feeding.

The dielectric Rogers RO4003 ($\varepsilon_r = 3.55$) is used in the feeding part and in the radiation middle part. This material has been chosen because it has a perfect value of dielectric permittivity in order to have a trade-off between bandwidth and beamwidth. If the effective dielectric permittivity is high, the patch dimension would be small and therefore the width of the radiation beam increases. However, the bandwidth depends inversely on the effective dielectric permittivity.

The dielectric Rogers RO3003 ($\varepsilon_r = 3$) has been chosen for the same reason of the RO4003. Moreover it has a better $\tan\delta$ and therefore less losses. Hence, the high effective dielectric permittivity is maintained while the efficiency of the antenna is not troubled.

Finally, the Rogers Prepreg 4403 ($\varepsilon_r = 3.17$) is used to bond the dielectric layers. This Prepeg has been chosen because its dielectric constant value. It has a similar dielectric permittivity value of RO3003. In this way the number of layers of Prepreg can be chosen in order to adjust the bandwidth. Stacking more Prepreg means a thicker dielectric and therefore more bandwidth. However, thick dielectrics decrease the efficiency of the antenna.

Dimension	Value (mm)	Dimension	Value (mm)
a	52.8	g	19.2
b	63.7	h	2
c	15	i	28.1
d	21	j	9.256
e	6.03	Microstrip Width	0.75
f	5.08	Copper Thickness	0

Table 3.1. Antenna dimensions

3.2.2. Impedance matching technique

In this point, the method used in this design for impedance matching is described. The software "SMITH v. 1.91" has been used to facilitate the calculation of the stub dimensions.

Once the upper patch is adjusted to resonate at 1.575 GHz, the decoupling stub is added. At an arbitrary distance of the probe (in this case 5 mm), a $\lambda/4$ stub with λ at 1.185 GHz is added in each feeding line of the HF-Port. Then another simulation is carried out. After the simulation, the results are deembedded to know the impedance (at 1.575 GHz) at the decoupling stub point. Afterwards, the impedance point is introduced in the application "SMITH v.1.92" in order to find the dimensions of the impedance matching stub.

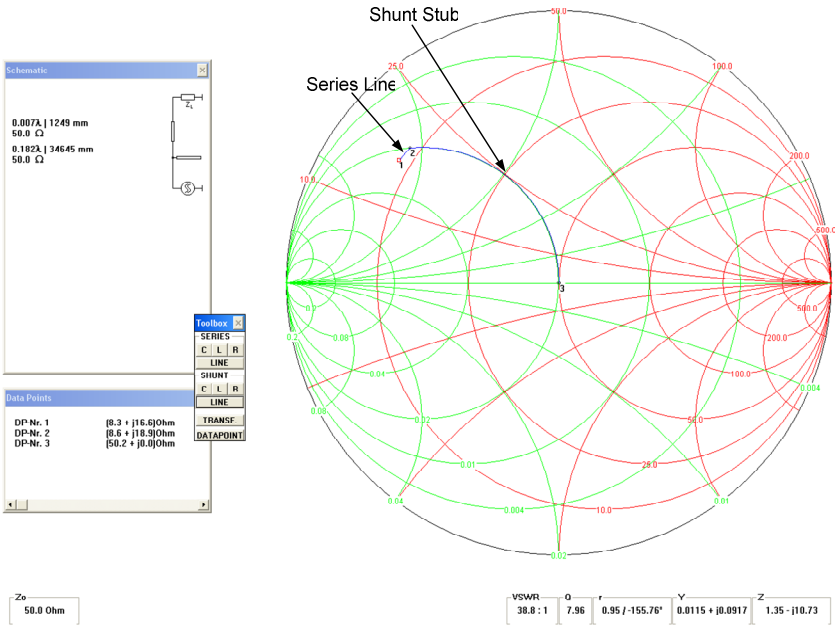

Figure 3.2. Example of impedance matching solution

The application's graphic interface is presented in Figure 3.2. In this image we can see an example of impedance matching. The original impedance is introduced in the application and adding one series line and a shunt stub the impedance can be transformed to 50Ω. In the left column, the dimensions of the stub are shown. The next step is to calculate the wavelength of the signal (at 1.575 GHz) in the microstrip layer with the aid of the "Estimator Tool" of Ansoft Designer 4.0. With all this information, the length of the series line and the shunt stub can be calculated and drawn in the layout.

In the LF-Port the same procedure has been followed, however the decoupling stub is not needed in this port because no coupling from this port to the other frequency has been shown.

3.2.3. Simulation results

In this section the results of the final simulation in Ansoft Designer 4.0 are presented. The simulations and adjustments made in Designer are not definitive, and therefore the values of the response do not completely match with the objectives.

The Figure 3.3 (a) shows the S-Parameters of one feeding line of each port. The HF band is completely covered by the HF-Port with an impedance match better than -10dB. However, the LF Band is not completely covered by the LF-Port. Nevertheless, this is not critical because what we are looking for is a sharp response in order to discriminate the frequencies off-band. Therefore, is better to adjust the antenna looking at the gain rather than the S-Parameters. The image (b) shows the coupling between LF and HF ports. This coupling is calculated measuring the signal power transferred from a feeding line of the LF-Port to the feeding line of the HF-Port that generates the same spatial mode in the antenna. For instance, if we look to Figure 3.1 this coupling coefficient would be the parameter S31 or the S24 of the antenna. The coupling level is under -25 dB in both bands and therefore we can say that both ports are complete decoupled.

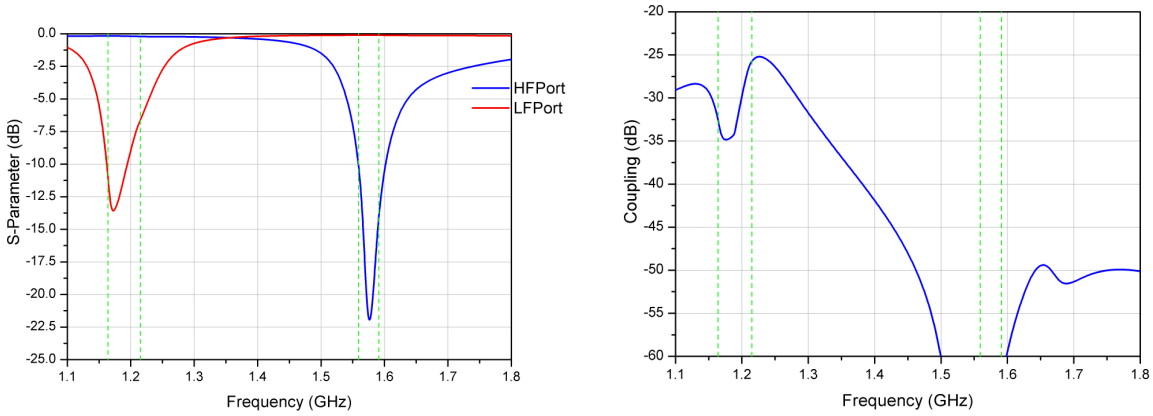

(a) (b)

Figure 3.3. (a) S-Parameters of the High Frequency Port and the Low Frequency Port (b) Coupling between the High Frequency Port and the Low Frequency Port

The gain of the antenna is presented in the Figure 3.4. The impedance mismatch has been taken into account only in the image (b). It has to be pointed out that the response is calculated separately for each port. The LF band response is obtained only exciting the LF-Port while maintaining the HF-Port matched to 50Ω and vice versa. The response would be almost the same if instead matching the opposite port, this is left to open circuit, since both ports are decoupled as seen before.

Can be noticed how the antenna behaves like two narrowband antennas radiating in RHCP. The crosspolar LHCP response is 15dB under the RHCP response, showing the good cross-polarization discrimination of the antenna.

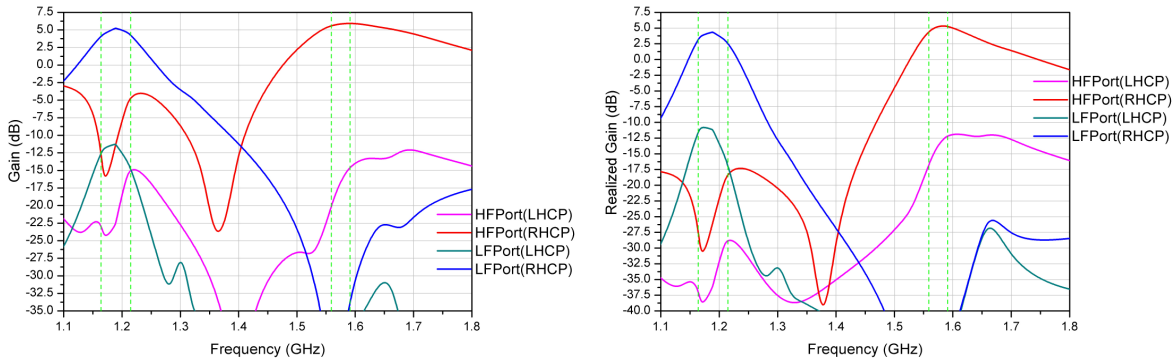

(a) (b)

Figure 3.4. Gain of the described antenna feeding both ports separately. Image (a) represents the accepted gain whereas (b) represents the realized gain.

The Figure 3.5 shows the Axial Ratio of the antenna exciting the LF-Port and HF-Port separately. Both responses are below 3 dB for the bands of interest.

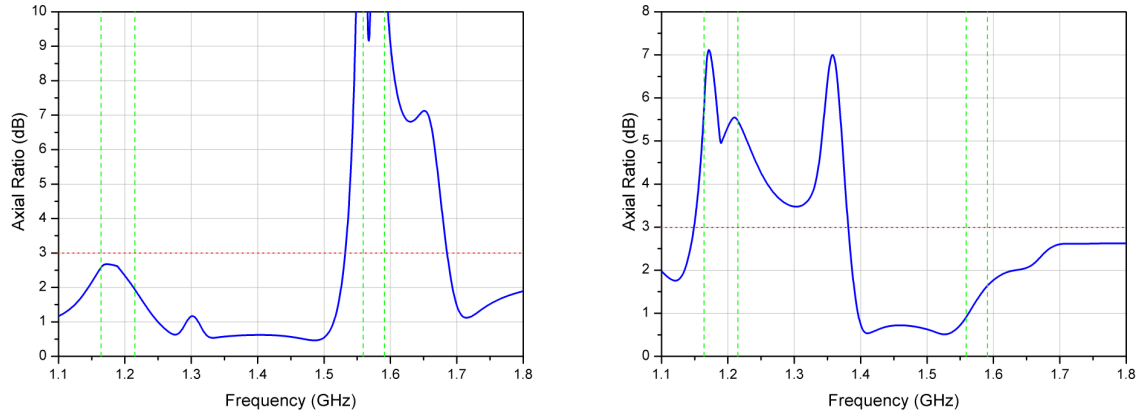

(a) (b)

Figure 3.5. Axial ratio of the described antenna. Image (a) represents the AR when feeding with the LF-Port while (b) represents the AR when feeding with the HF-Port

The Figure below presents the coupling between the feeding lines of each port. The image (a) and (b) show the coupling of the LF-Port and HF-Port respectively. The level of coupling of the HF-Port is below -20 dB, and therefore the feeding lines can be considered decoupled. However, the coupling level of the LF-Port is about -13dB at its maximum. This effect can lead to a bad axial ratio when inserting the 90° Hybrid.

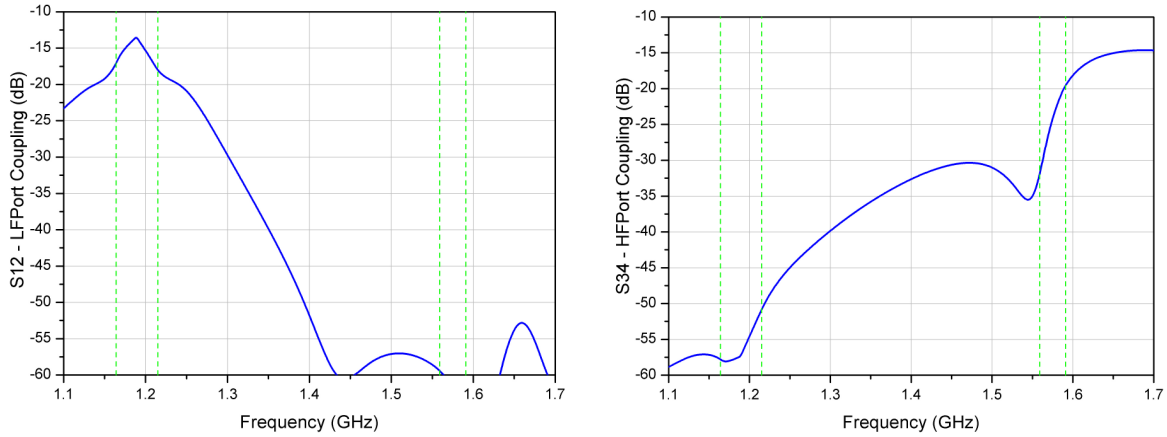

(a) (b)

Figure 3.6. Coupling between feeding lines of (a) LF-Port and (b) HF-Port

The radiation patterns of the antenna are presented in the Figure 3.7. We can notice how both patterns do not fulfil the requirements because the gain at 85° in elevation is very low. However, we should not forget that Ansoft Designer 4.0 works with an infinite ground plane avoiding any possible field diffraction to the low hemisphere ($90 \leq \theta \leq 180$). Hence, these results are not precise and the antenna should be simulated in Ansoft HFSS 11 in order to take into account that the structure is finite.

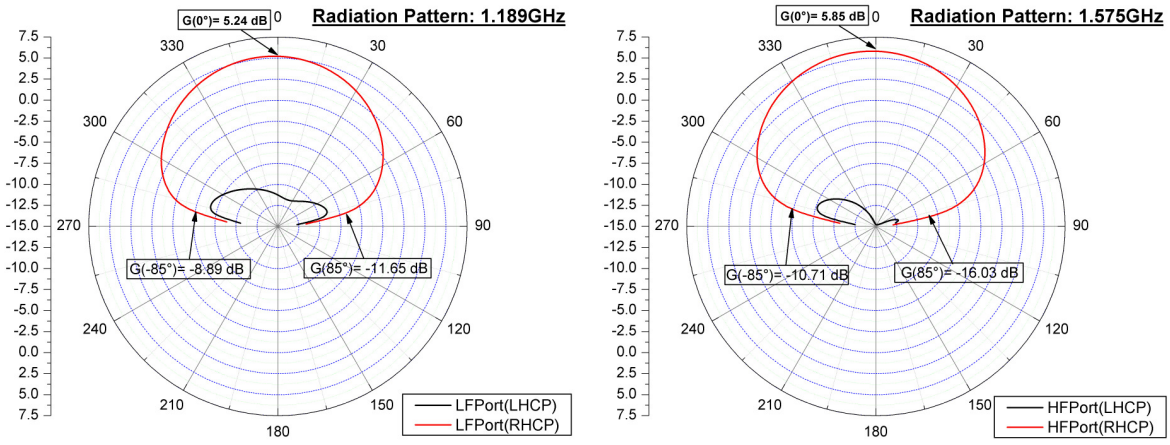

(a) (b)

Figure 3.7. Radiation patterns of the described antenna. Image (a) shows the radiation pattern of the low band and image (b) shows the radiation pattern of the high band.

3.3. *Final adjustment in HFSS*

The next step is to simulate the antenna geometry in Ansoft HFSS 11 in order to have a better precision in the calculation of the electromagnetic fields.

3.3.1. Antenna geometry

The dimensions of the antenna are exactly the same with only three changes respect point 3.2: the dimension of the bottom patch, the finite structure and the copper thickness. Now the dielectric geometry measures $95x95mm$ and the feeding lines are adjusted in length in order to place the waveports in the edges of the dielectrics.

The antenna geometry is presented in Figure 3.8, showing the top view of finite 3D structure in image (a) and the layer stack-up in image (b).

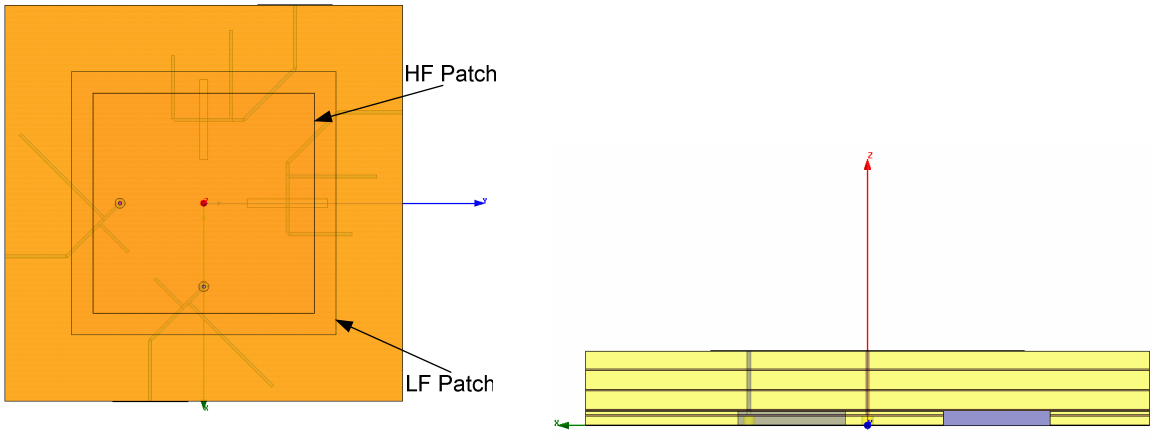

(a) (b)

Figure 3.8. (a) Top view and (b) side view of the antenna geometry

In this model, the copper thickness has been chosen to be 35 um in order to take into account the losses of the conductor. Furthermore, the bottom patch dimension has been modified to adjust the LF resonance. The new bottom patch side dimension is 63,1 mm

In the image below a perspective view of the antenna is presented just to have an insight of how will be the antenna geometry in reality.

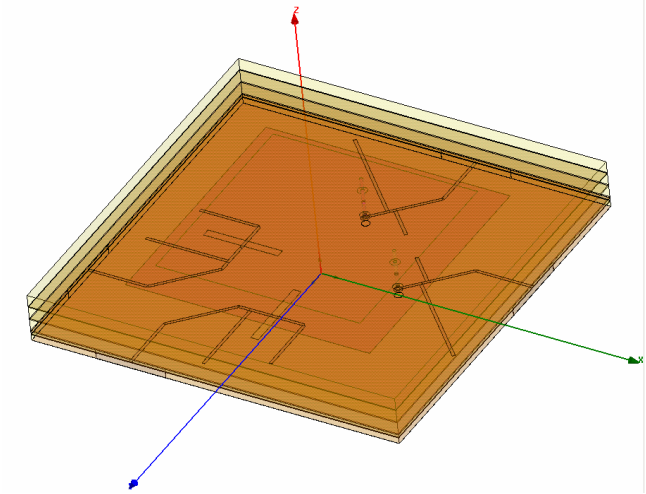

Figure 3.9. Perspective view of the antenna geometry

3.3.2. Simulation results of the low band

Two kinds of simulations have been carried out with the antenna. One simulation has been made with the mesh adaptation centered to 1.189 GHz in order to adjust the low frequency part of the antenna. Moreover, another simulation with the mesh adaptation centered to 1.575GHz has been made to adjust the antenna high frequency part. In this section are explained the results of the antenna obtained exciting only the LF-Port and running a simulation with the mesh being calculated to have the minimum error at 1.189 GHz.

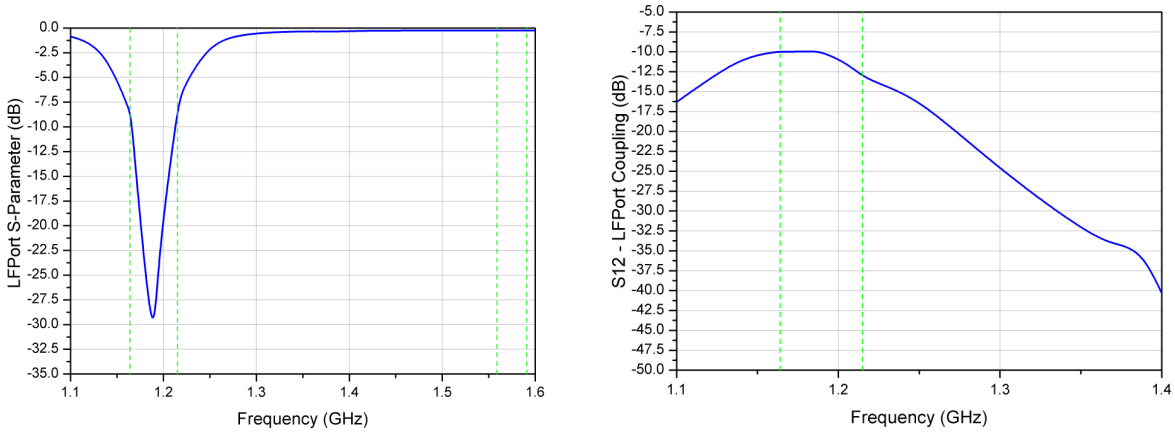

(a) (b)

Figure 3.10. (a) Reflection coefficient of the LF-Port.
(b) S12 coupling between the two feeding lines of the LF-Port

The reflection coefficient and the coupling between feeding lines are presented in the Figure above. We can see how the entire low frequency band is under -8 dB of impedance matching, which means that in the boundary of the band the 16% of the power is reflected. In the table below the significant values of the Figure 3.10 are shown. With a coupling of -10 dB the feeding lines are not completely decoupled and it could cause problems in the axial ratio when inserting the 90°-hybrid.

Frequency (GHz)	LF-Port R.C. (dB)	LF-Port Coupling (dB)
1.164	-8.41	-10.01
1.189	-34.46	-9.96
1.215	-8.04	-13.06

Table 3.2. Significant values of the return loss and coupling of the LF-Port

The level of coupling between LF-Port and HF-Port is presented in Figure 3.11. The values are not precise outside the low band because the mesh is optimized only for the low band, but we can have an insight of the values of coupling. Actually, those values are very low and this can be understood like both ports are completely decoupled. The maximum value of coupling inside the low band is at f=1.215GHz is -25dB that means that a 0.32% of power is coupled from one port to the other at this frequency. This value is insignificant.

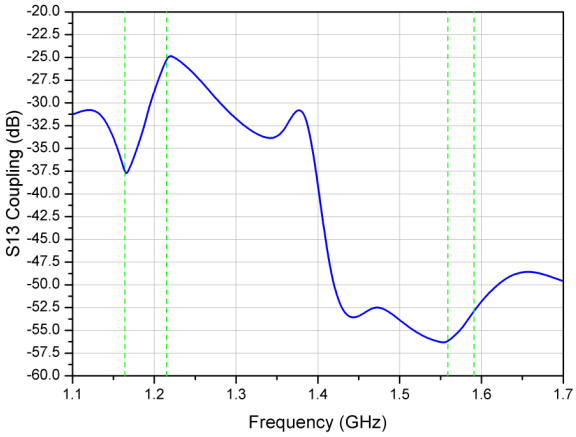

Figure 3.11. Coupling between LF-Port and HF-Port

The images below present the gain and the axial ratio of the antenna exciting the LF-Port. The gain response is narrow band, centered in 1,189 GHz. Furthermore, can be noticed from the image (a) how the level of radiation in the high frequency band is very low (around -28 dB). The impedance mismatch has been taken into account only in the realized gain curves. By other hand, we have to point out that the axial ratio in the whole low frequency band is below 3dB.

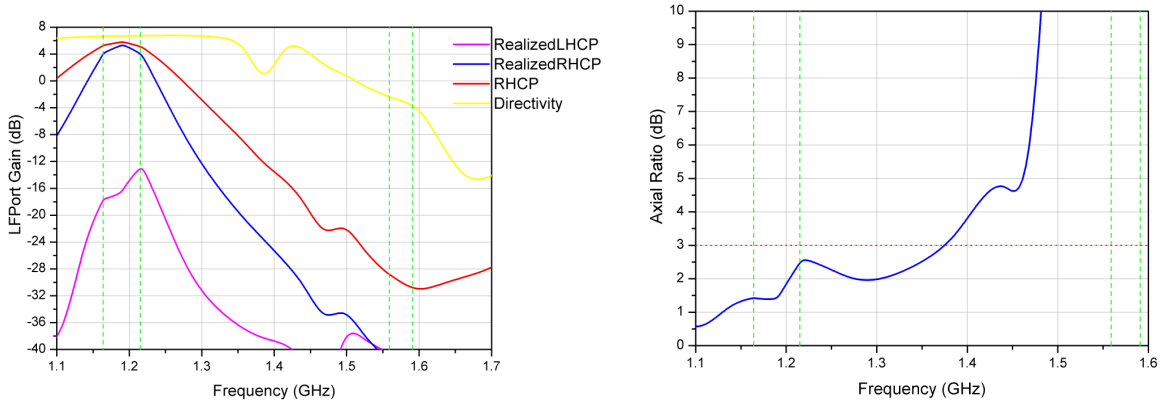

(a) (b)

Figure 3.12. (a) Gain of the antenna exciting the LF-Port.
(b) Axial ratio of the antenna exciting the LF-Port

The Table 3.3 shows the values of the gain in the significant points of the low band. The maximum gain is in the center of the band and corresponds to 5.33dB. Moreover, from these values we can obtain that the maximum difference of gain in the band is 1.18 dB. This variation can be equalized completely by the receiver.

Frequency (GHz)	Realized Gain. (dB)
1.164	4.23
1.189	5.33
1.215	4.15

Table 3.3. Significant gain values exciting the LF-Port

The images below present the radiation patterns of the low band. The graph (a) shows the radiation patterns for 0° and 90° cuts of Phi at the center frequency of the band. Both cuts have almost the same response, showing a good low elevation gain with values of -3 dB and -4.95 dB of gain at 85° of elevation. Those values of gain are enough to satisfy our requirements. The asymmetry of the patterns is due to the asymmetric feeding of each band.

By other hand, in the image (b) a comparison among the radiation patterns of the three significant frequencies is presented. The three curves have the same shape, being the variation in gain the only difference among them.

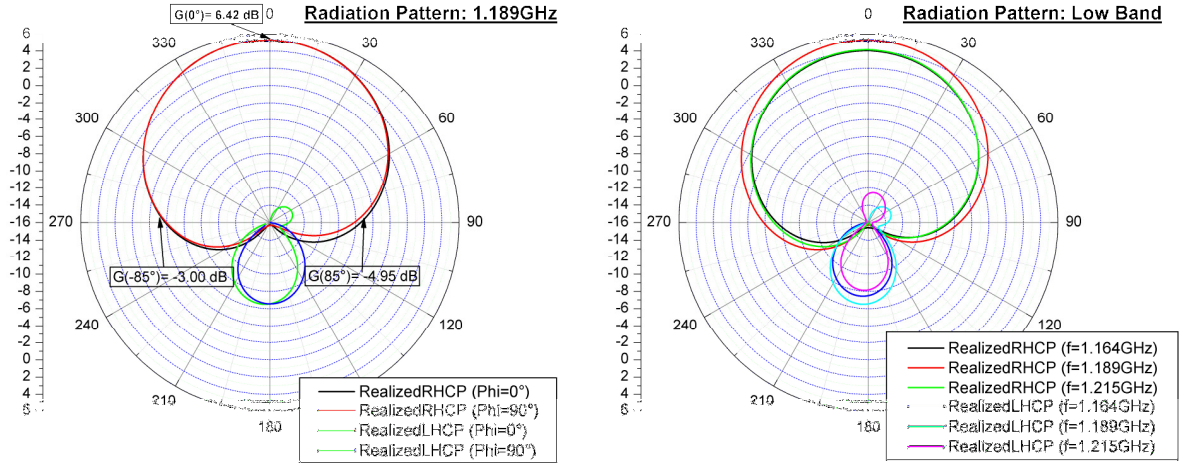

(a) (b)

Figure 3.13. (a) Radiation pattern at the center frequency of the low band. (b) Comparison of the radiation pattern in the center frequency and at the border frequencies of the low band.

3.3.3. Simulation results of the high band

This simulation has been carried out adapting the mesh in order to have the minimum error at 1.575 GHz. Moreover only the HF-Port is excited in order to only have the response of the fields created by the HF part of the antenna. In this simulation the LF-Port is loaded with 50 Ohm.

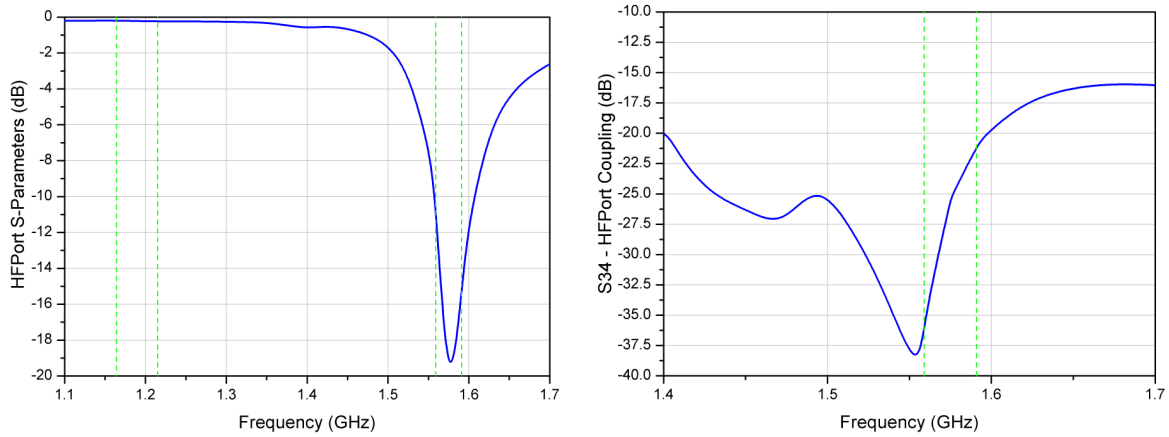

(a) (b)

Figure 3.14. (a) Reflection coefficient of the HF-Port
(b) S34 coupling between the two feeding lines of the HF-Port

The impedance matching curve and the coupling level between the two feeding lines of the HF-Port are presented in the Figure above. The HF band is completely matched below -10 dB. Moreover, the maximum coupling in the band is -20 dB, enough to consider that both feeding lines of the HF-Port are decoupled. In the table below are shown the significant values of the Figure 3.14.

Frequency (GHz)	LF-Port R.C. (dB)	LF-Port Coupling (dB)
1.559	-10.11	-35.29
1.575	-22.17	-25.51
1.591	-15.33	-21.079

Table 3.4. Significant values of return loss and coupling in the HF band

The Figure 3.15 presents the gain and the axial ratio of the HF band. Like in the LF band, the response in the HF band of this antenna is narrow band, with an enough bandwidth to cover the entire band. It has to be pointed out how the efficiency of the antenna in this band is high (91.6%), since the gain and the directivity in the center of the band only differ 0.38 dB.

The axial ratio in this band is presented in the image (b) of the Figure 3.15. The level of axial ratio is below 2 dB in the whole band. This good value of axial ratio is translated in a difference of 19 dB between the copolar and crosspolar field components.

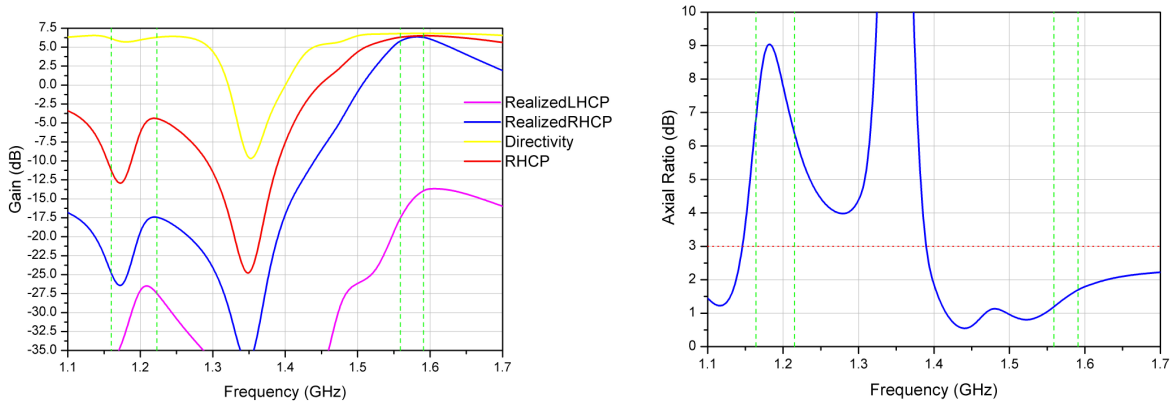

(a) (b)

Figure 3.15. (a) Gain of the antenna exciting the HF-Port.
(b) Axial ratio of the antenna exciting the HF-Port

In the following table are shown the significant values of the gain in the HF band. The maximum difference in gain is 0.56 dB for the whole band.

Frequency (GHz)	Realized Gain. (dB)
1.164	5.86
1.189	6.42
1.215	6.34

Table 3.5. Significant values of gain in the HF band

The radiation patterns of the high band are presented in the Figure 3.16. The image (a) shows the patterns for 0° and 90° cuts of Phi at the center frequency of the band. Both cuts have almost the same response, showing a very good low elevation gain with values of -2.16 dB and -4.18 dB at 85° of elevation. Those values of gain satisfy our requirements. These radiation patterns have the same problem as the LF band patterns: they are asymmetric. The reason is the identical as in the LF band, the feeding is asymmetric.

In the image (b) a comparison among the radiation patterns of the three significant frequencies of the HF band is presented. Again, the three curves have the same shape, being the variation in gain the only difference among them.

From these results together with the LF band results can be noticed how this antenna have a radiation patterns that are adapted perfectly to our needs. When building the array, the asymmetry can be compensated by using a sequential shift placement of the antennas.

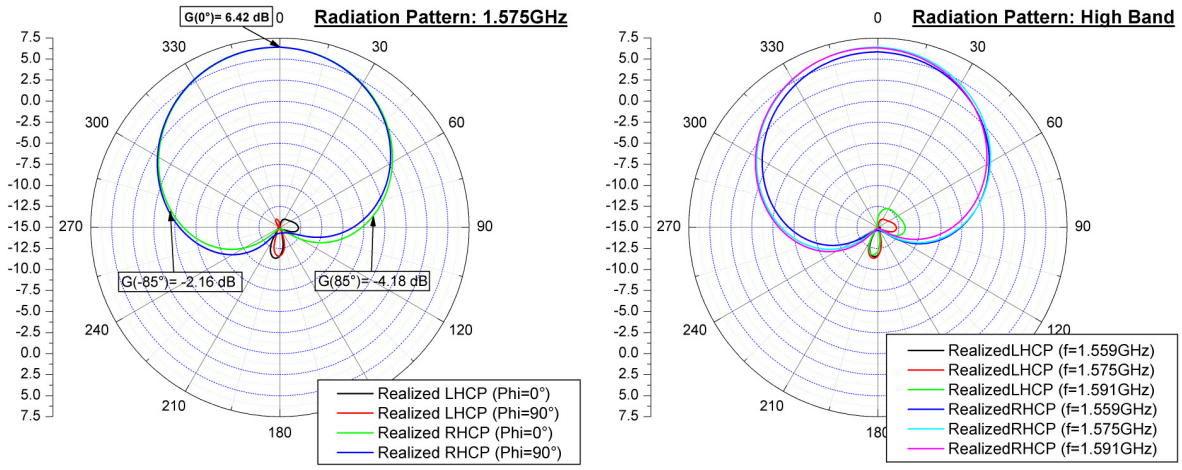

(a) (b)

Figure 3.16. (a) Radiation pattern at the center frequency of the high band. (b) Comparison of the radiation pattern at the center frequency and at the border frequencies of the high band.

3.4. Parameter sweep

In this section a parametric sweep has been carried out with the intention of studying the influence of the feeding components dimensions in the antenna response. A total number of three sweeps have been made: the slot length, the slot position and the probe position have been varied in order to find the optimum value of each. This information will be useful to understand and modify the antenna for further prototypes. Hence, if the measurements of the first prototype do not fulfil the objectives, this information will be useful to make the necessary adjustments. It has to be pointed out that all the modifications are made from the original values of the antenna of section 3.2.

3.4.1. Slot length

The Figure 3.17 presents the variation of the reflection coefficient of one feeding line of the LF-Port with the modification of the slot length from 15 mm to 25 mm. We can notice how as the length increases, the slots become resonant at the frequency of interest and therefore the bandwidth of the antenna increases. However, although is not presented in the next Figures, it should be pointed out that the efficiency of the antenna will decrease if the slot length increases due to the back radiation.

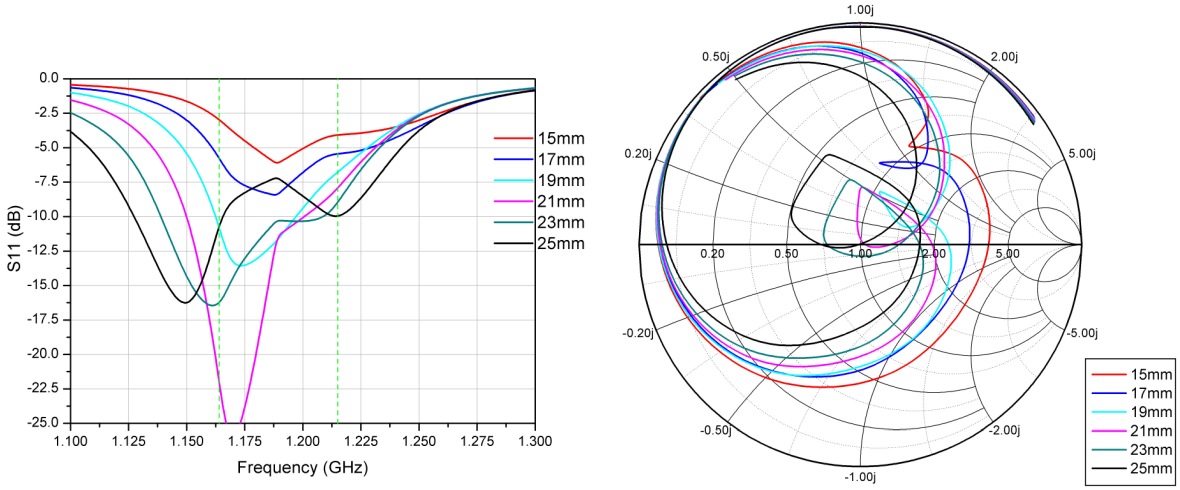

(a) (b)

Figure 3.17. Return loss of the LF-Port. Image (a) shows a rectangular graph in dBs whereas image (b) shows the variation of the S11 in the Smith Chart.

In the image below the coupling between feeding lines of the LF-Port is presented. We can see how the minimum level of coupling is achieved with a length of 15 mm while the maximum is associated with a length of 19-20 mm.

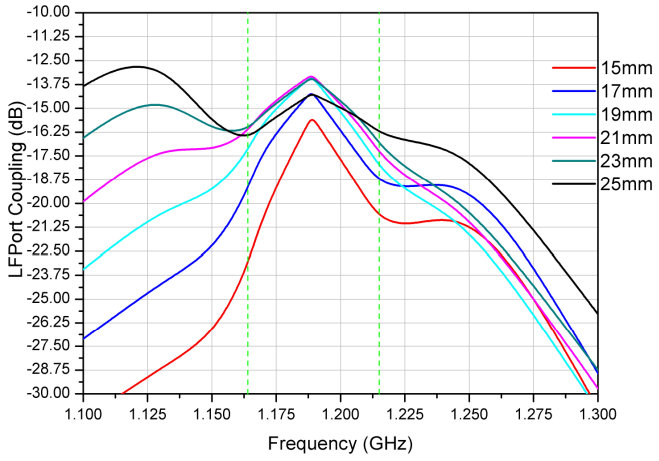

Figure 3.18. Coupling between the LF-Port and the HF-Port.

The Figure 3.19 shows the variation of the axial ratio with respect to the slot length. The minimum level of axial ratio is achieved with the maximum length of the slot whereas the maximum level is obtained with the minimum slot length.

In this section can be noticed how increasing the slot length the axial ratio and the coupling can be improved. Moreover, the bandwidth can be increased with the same change in the slot length. If any of these parameters has a bad response when measuring the prototype, a possible change would be increasing the slot length.

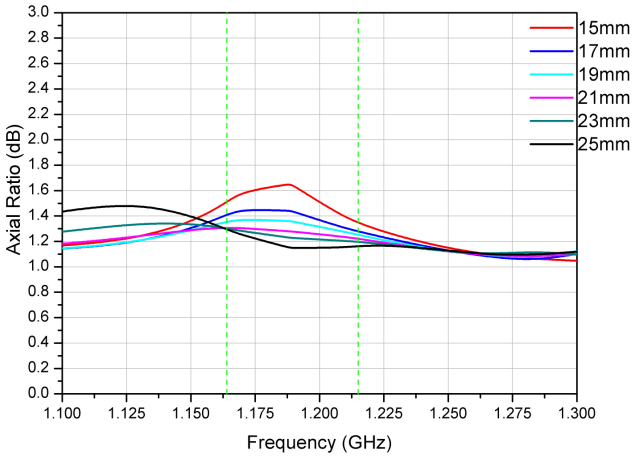

Figure 3.19. Axial ratio of the low frequency band feeding the LF-Port

3.4.2. Slot position

The Figure 3.20 presents the variation of the reflection coefficient of one feeding line of the LF-Port with the modification of the slot mid point distance from the center of the antenna. This distance is swept from 15mm to 25mm. As can be seen in the Figure, this change in position of the slots does not change the input return loss of the LF-Port, since all the curves almost completely overlap.

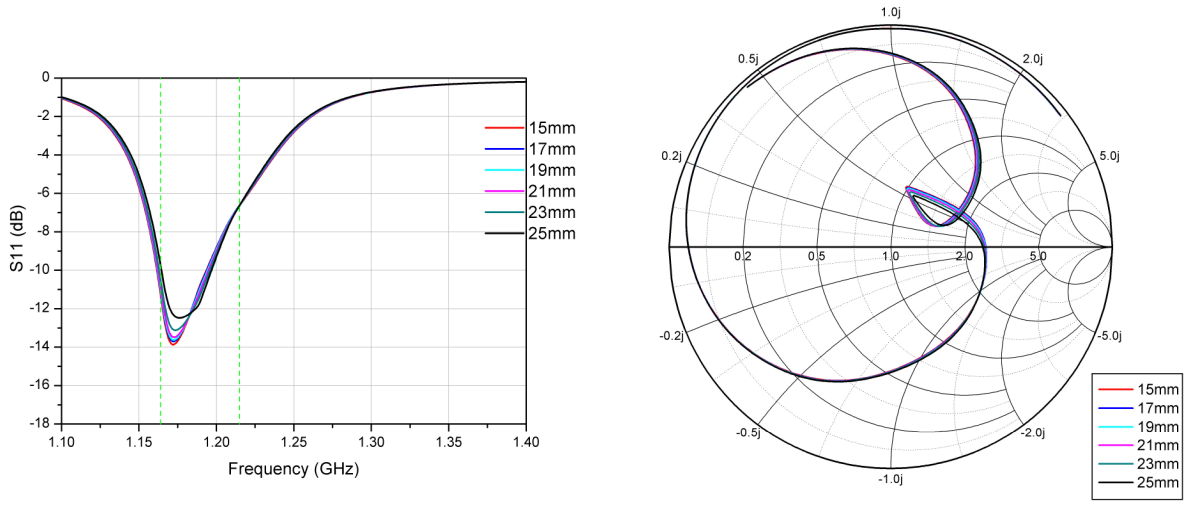

(a) (b)

Figure 3.20. Reflection coefficient of the LF-Port. Image (a) shows a rectangular graph in dBs whereas image (b) shows the variation of the S11 in the Smith Chart.

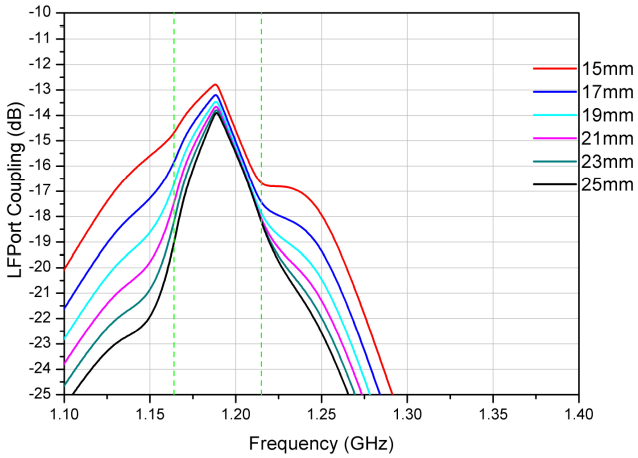

Figure 3.21. Coupling between the LF-Port and the HF-Port

In the image above the coupling between feeding lines of the LF-Port is shown. We can see how the minimum level of coupling is achieved with a displacement of 25 mm while the maximum is associated with a length of 15 mm.

The Figure 3.22 shows the variation of the axial ratio with respect to distance of the mid point of the slot to the center of the antenna. The lowest level of axial ratio is achieved with the minimum distance while the highest level of axial ratio is obtained with the maximum distance to the center.

From this analysis, it can be concluded that the optimum distance is around 19 mm. Moreover, the variation of this parameter is not recommended, since there is a trade-off between axial ratio and LF-Port coupling that should be maintained.

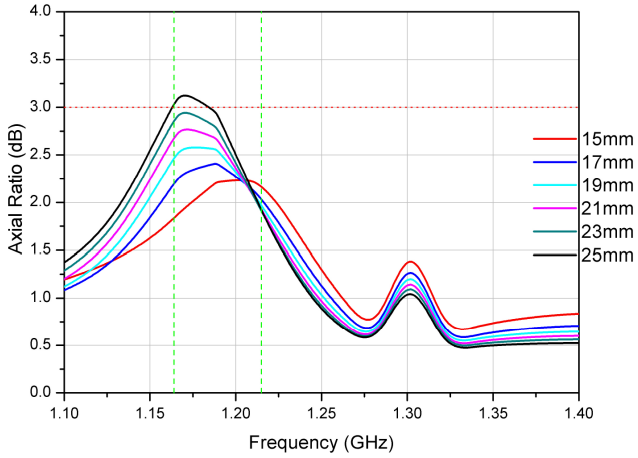

Figure 3.22. Axial ratio of the low frequency band feeding the LF-Port

3.4.3. *Probe position*

The Figure 3.23 presents the variation of the return loss of one feeding line of the HF-Port with the modification of the probe distance from the center of the antenna. This distance is swept from 15mm to 25mm. The impedance matching bandwidth of the antenna increases if the slot is displaced towards the border of the antenna.

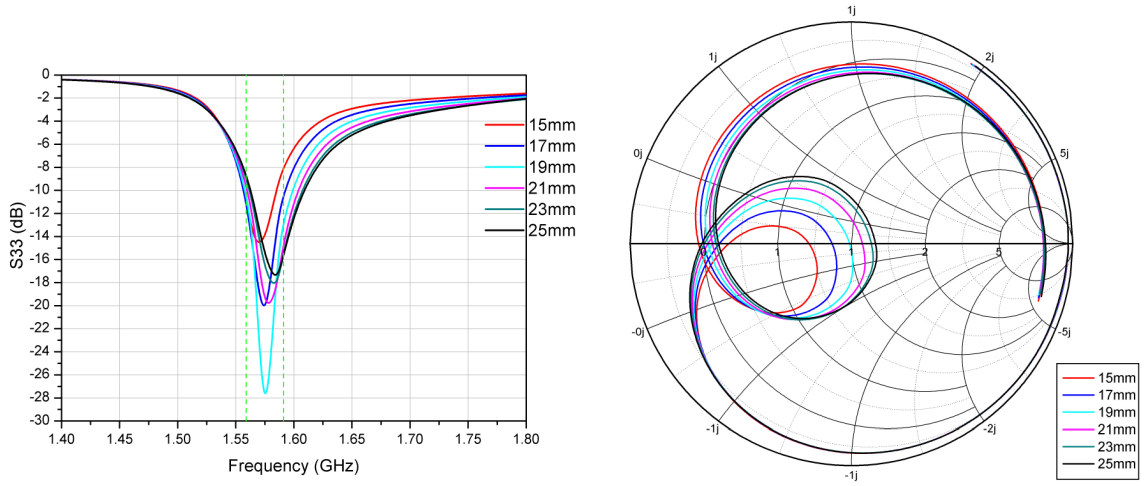

Figure 3.23. Return loss of the HF-Port. Image (a) shows a rectangular graph in dBs whereas image (b) shows the variation of the S11 in the Smith Chart.

In the image below we can se the variation of the coupling in the LF-Port. It has to be pointed out how the variation of the probe position affects directly to the coupling of the LF-Port. The closer is the probe of the center of the antenna; the lower is the coupling in the LF-Port.

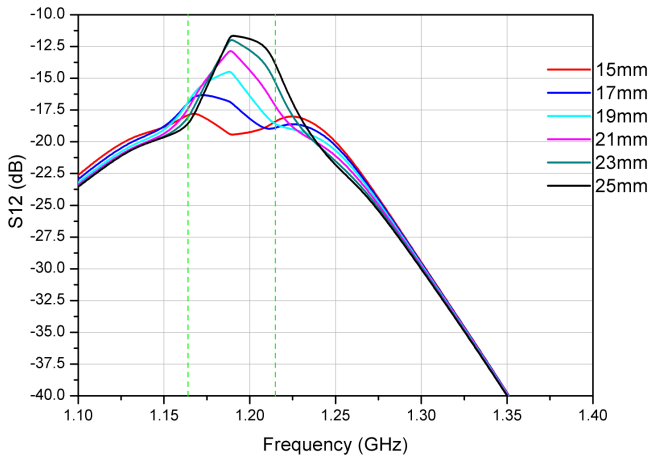

Figure 3.24. Coupling between the feeding lines of the LF-Port

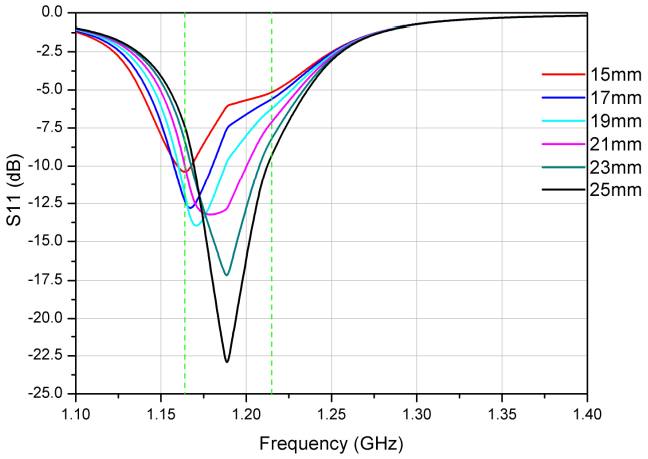

Figure 3.25. Return loss of the LF-Port

The Figure 3.25 shows the variation in the reflection coefficient of the LF-Port. From this Figure we can see how the further is the probe from the center of the antenna; the bigger is the bandwidth in the LF band.

By other hand, in the Figure below is presented the variation of the axial ratio in both ports. The trend in the variation is the same for the LF-Port and the HF-Port. The axial ratio is improved if the distance of the probes to the center of the antenna decreases.

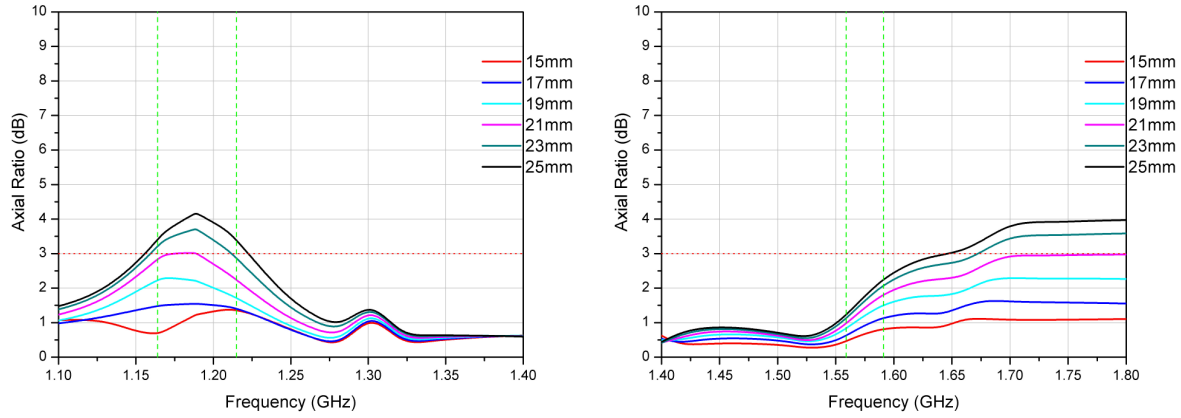

Figure 3.26. Axial ratio of the low frequency band feeding the LF-Port (a) and of the high frequency band feeding the HF-Port (b)

From the graphs presented above, we can conclude that that in the case of having a bad result either in the measurement of the axial ratio or the LF-Port coupling, the probe can be displaced towards the center of the antenna and afterwards, try to adjust the impedance matching.

3.5. Antenna construction and measurements

Once the antenna has been adjusted in HFSS and fulfils all the objectives, the construction of the first prototype is carried out.

3.5.1. Construction of the antenna

First the process of patterning/imaging is carried out to draw the patches, the feeding lines and the slots to their respective dielectric layers. Afterwards, the lamination process is made in order to bonding together the dielectrics layers. Then the drills are made and plated with copper. Finally the connectors are soldered to the corresponding feeding lines. The result is shown in Figure 3.27 (a).

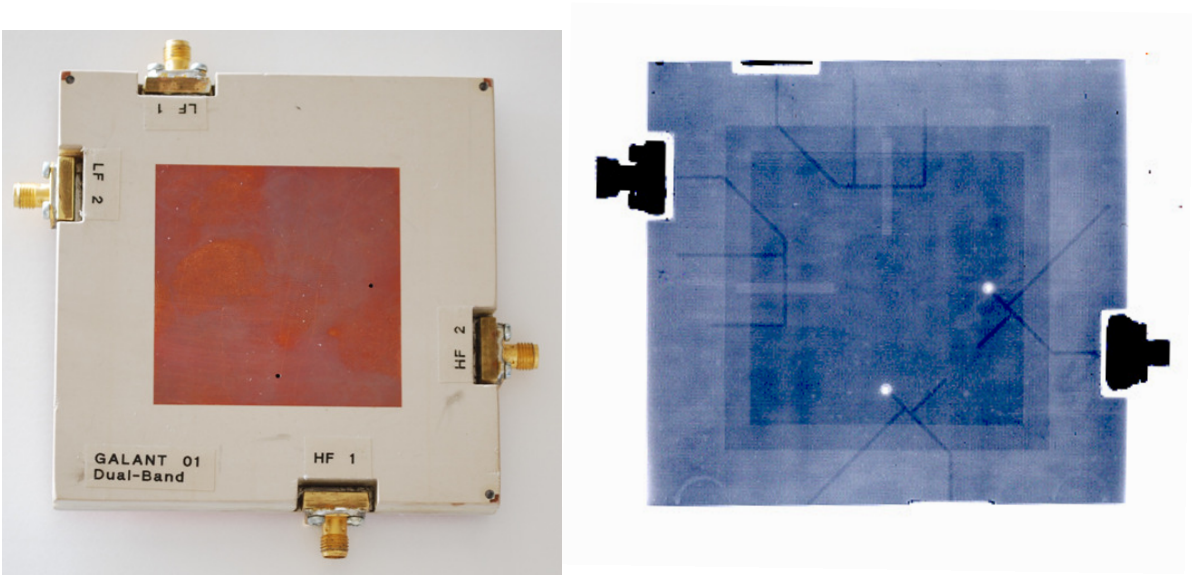

(a) (b)

Figure 3.27. (a) Photograph of the build antenna.
(b) X-Ray photograph of the built antenna.

Figure 3.27 (b) shows an X-Ray photograph of the antenna. This picture was taken in order to check if the antenna was constructed properly. Both patches and the feeding lines can be observed in their right positions.

3.5.2. Measurements

The S-Parameters of the antenna have been measured using the network analyzer shown in the Figure 3.28.

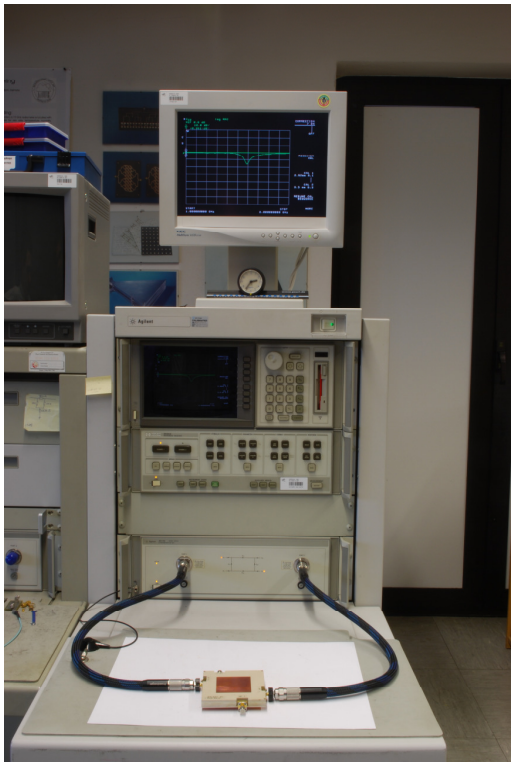

Figure 3.28. Network analyzer at the Antenna Group laboratory

In the Figure below the measured S11 (LF-Port) parameter is shown. The result is different from what we expected. Basically it seems like the antenna is unmatched, but the resonance of the bottom patch is correct.

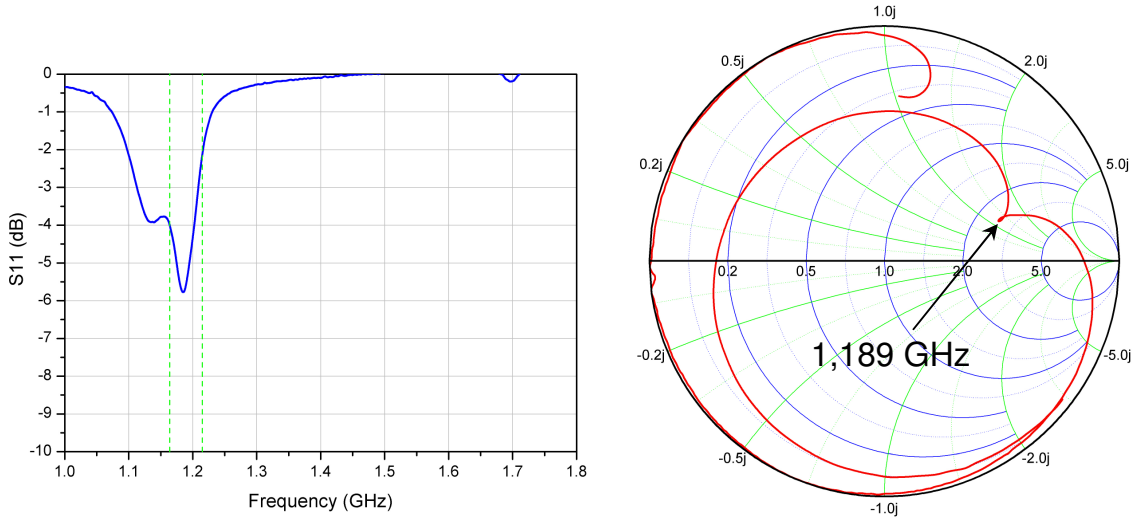

(a) (b)

Figure 3.29. Measured S11 presented in a rectangular plot (a) and in a smith chart (b).

The Figure 3.30 presents the measured S33 (HF-Port) of the antenna. The impedance matching of this port is correct. A slight shift in the resonance can be noticed. This problem could be solved just adjusting the dimension of the top patch.

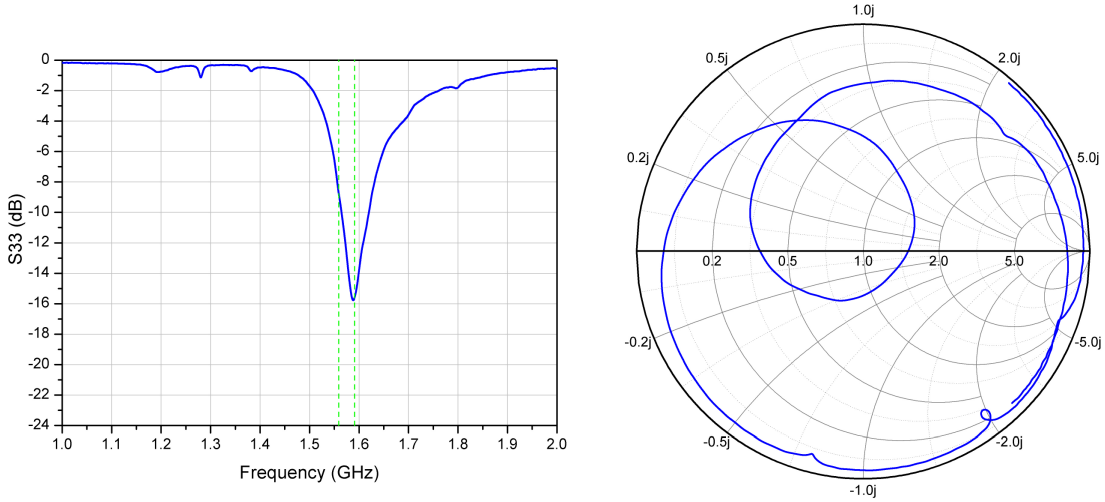

(a) (b)

Figure 3.30. Measured S33 presented in a rectangular plot (a) and in a smith chart (b).

From this results can be concluded that there is a problem in the feeding layer. The radiation part of the antenna seems to be correct, but there is an error in the permittivity of the stripline dielectrics. In the HF-Port is harder to notice the effect because the loop in the Smith Chart is wide enough not to vary the response of the return loss.

3.5.3. Identification of the problem

In the picture below is shown a comparison between the simulated and measured isolation between ports. In both curves there is a peak created by the decoupling stubs close to the LF-Band. This peak is displaced 50 MHz in the measured curve from the simulated curve.

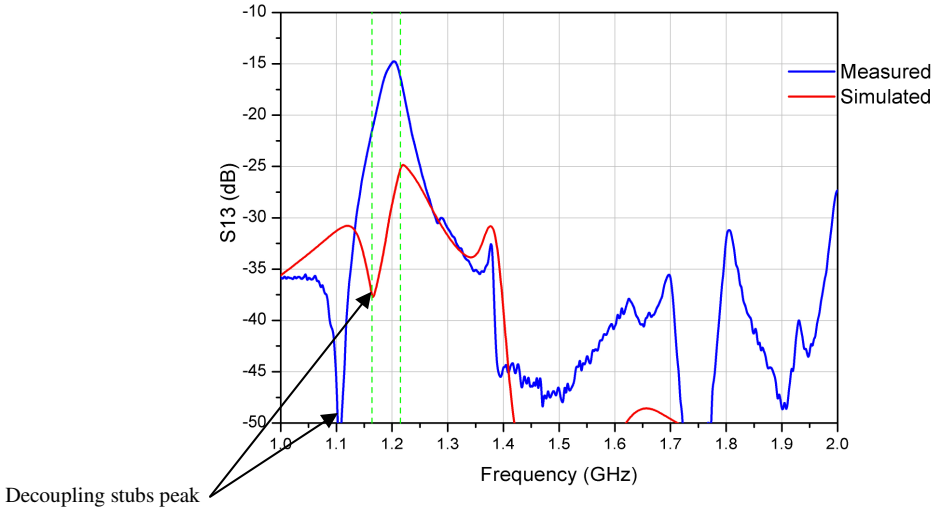

Figure 3.31. Comparison between simulated and measured isolation between ports

With the position of the peak and the length of the slot we can estimate the stripline effective permittivity. The peak is situated at 1.105 GHz and the length of the stub is 28.1 mm. Knowing that the stub has a length of $\lambda/4$ at the peak frequency:

$$\lambda_{1.105GHz} = 28.1 \cdot 4 = 112.4mm \tag{3.1}$$

And then we can estimate the ε_{eff} :

$$112.4 \cdot 10^{-3} m = \frac{300 \cdot 10^6 m/s}{1.105 \cdot 10^6 s^{-1} \cdot \sqrt{\varepsilon_{eff}}} \text{; From here we obtain a } \varepsilon_{eff} = 5.83 . \tag{3.2}$$

The effective permittivity obtained with Ansoft Designer, using the current dielectric layers in the stripline is 5. Therefore, the hypothesis is that the wrong results are caused by an important shift in the effective permittivity in the stripline.

We can test the hypothesis adjusting the effective permittivity of the stripline to 5.8 and simulate the antenna to check whether the results match.

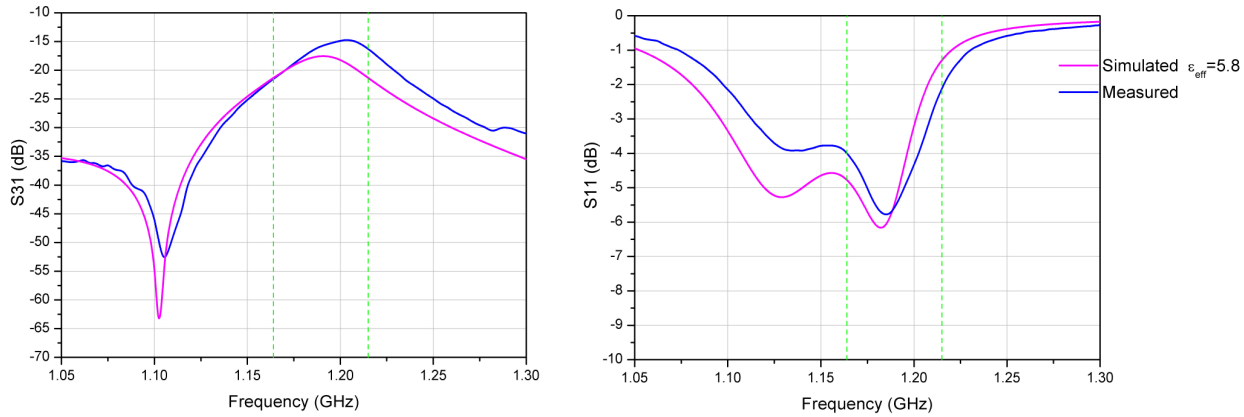

(a) (b)

Figure 3.32. Comparison between the S31 (a) and S11 (b) measured and simulated with $\varepsilon = 5.8$.

In the Figure above the similarity between both measured and simulated results can be observed. The HF-Port response has been also checked and the behaviour is the same. In this port, the response in the smith chart is shifted but the loop is wide enough to not change drastically the matching of the antenna.

Now there is still work to find out what can produce a shift of 0.8 in the effective permittivity. It is a drastic change, since the value of the bottom dielectric should have changed from 3.5 to 5.2. This change is completely outside the tolerances given by the dielectric manufacturer.